Supplementary Information

Boosting Circularly Polarized Luminescence by Optimizing Off-Centering Octahedral Distortion in Zero-Dimensional Hybrid Indium-Antimony Halide

Yulian Liu[1], Yi Wei[1], Zhishan Luo[1], Bin Xu[1], Meiying He[1], Peibin Hong[1], Chen Li[1], Zewei Quan[1]*

[1]Department of Chemistry, and Academy for Advanced Interdisciplinary Studies, Southern University of Science

*Correspondence: quanzw@sustech.edu.cn

Experimental section

Materials

Chemicals listed below are commercially available and used without further purification. *R*-methylbenzylamine (*R*-MBA, TCI, 98%), *S*-methylbenzylamine (*S*-MBA, TCI, 98%), dimethylamine hydrochloride (2MA, 99%, Meryer), trimethylamine hydrochloride (3MA, TCI, > 97%), indium chloride ($InCl_3$, 99.99%, Meryer), antimony chloride ($SbCl_3$, 99.99%, Meryer), hydrochloric acid (HCl, 38 wt. % in H_2O, Shanghai Lingfeng Chemical Reagent), N,N-dimethylformamide (DMF, 99.9%, Aladdin) and potassium bromide (KBr, SP, Aladdin). Two-part PDMS DC184 encapsulant (Dow-Corning) were used.

Synthesis of *R*/*S*-1 single crystals.

3mmol of 2MA, 1.8 mmol of *R*/*S*-MBA, 1.44 mmol of $InCl_3$, 0.06 mmol of $SbCl_3$, and 1 mL of concentrated HCl were mixed and heated up to 100 ℃ until dissolved. *R*/*S*-1 single crystals can be obtained by slowly cooling the mixed solution to room temperature. Undoped single crystals of $(R/S\text{-MBA})_2$2MA$InCl_6$ were synthesized through the same procedure as *R*/*S*-1, except that 1.44 mmol of $InCl_3$ and 0.06 mmol of $SbCl_3$ were replaced with 1.5 mmol of $InCl_3$.

Synthesis of *R*/*S*-2 single crystals.

The synthesis of *R*/*S*-2 is the same as *R*/*S*-1, except that the 3 mmol of 2MA was replaced by 3 mmol of 3MA. Undoped $(R/S\text{-MBA})_2$3MA$InCl_6$ single crystals were synthesized through the same procedure as *R*/*S*-1, except that 1.44 mmol of $InCl_3$ and 0.06 mmol of $SbCl_3$ were replaced with 1.5 mmol of $InCl_3$. The synthesis of *R*/*S*-2A, *R*/*S*-2B, and *R*/*S*-2C is the same as the procedure of *R*/*S*-2, except that 1.44 mmol of $InCl_3$ and 0.06 mmol of $SbCl_3$ were replaced by 1.28 mmol of $InCl_3$ and 0.22 mmol of $SbCl_3$ for *R*/*S*-2A, 1.1 mmol of $InCl_3$ and 0.4 mmol of $SbCl_3$ for *R*/*S*-2B, and 1 mmol of $InCl_3$ and 0.5 mmol of $SbCl_3$ for *R*/*S*-2C, respectively.

Fabrication of UV-Pumped LED.

First, *R*/*S*-2C was grounded into powder and mixed with PDMS and curing agent. Then, the mixture was coated on a 365 nm ultraviolet GaN LED chip. The devices were further cured at 100 ºC for 4 hours.

Characterizations

SCXRD data were collected using a Bruker D8 Venture X-ray single crystal diffractometer equipped with molybdenum (Mo Kα = 0.71073 Å) sealed tube as the X-ray source. SCXRD characterizations were performed at 100 K. The structures were solved using the SHELXT structural solution program and refined by the SHELXL refinement package using the least-squares minimization.[1, 2] All atoms were refined anisotropically. PXRD results were obtained using an X-ray powder diffractometer (Rigaku SmartLab) equipped with Cu Kα radiation (λ = 0.15418 Å) at 45 kV and 200 mA. The scanning speed was 10° min^{-1}. ICP-MS characterizations were conducted using an Agilent 7700x. UV-Vis absorption spectra were collected on a UV-3600i Plus spectrophotometer with $BaSO_4$ as the reference substance. PL, PLE spectra, and PLQYs were measured at room temperature on an Edinburgh FLS1000 spectrometer equipped with a xenon lamp (450W) as the excitation source. PL lifetimes were measured on Edinburgh FLS1000 spectrometer using a 310 nm VP-LED and a 280 nm EPL-LED as excitation sources. Power-dependent PL spectra were monitored using a Thorlab PM100D power meter with a standard photodiode power sensor (S120VC). CD spectra were measured for powder samples in KBr pellets using an Applied Photophysics Chirascan spectrometer at a scan speed of 1 nm/s. The KBr pellets for CD characterizations were prepared in two steps. First, 5 mg of each compound and 90 mg KBr were mixed and grounded into powders. Then, a 13 mm diameter pellet die was used to press powders into pellets under 12 MPa. CPL spectra were collected for thin films on quartz plates using a JASCO CPL-300 instrument. The films for CPL testing were prepared by dispersing the HMHs solution (31% wt in DMF, 20 μL) onto quartz glass substrates (diameter of 2 cm), followed by annealing at 100 °C for 30 min. EL

spectra were collected using a LED integrated test system HAAS-2000.

Supplementary figures

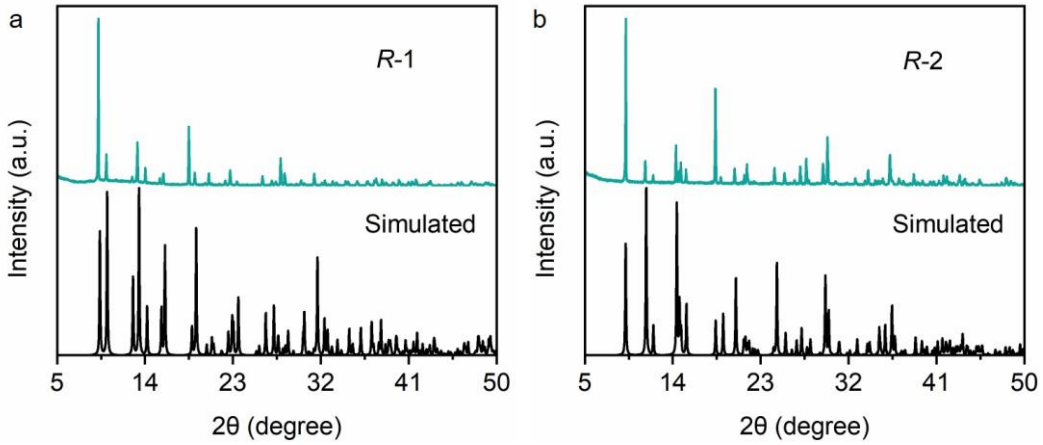

Figure S1. (a-b) Experimental and simulated PXRD patterns of *R*-1 and *R*-2, respectively.

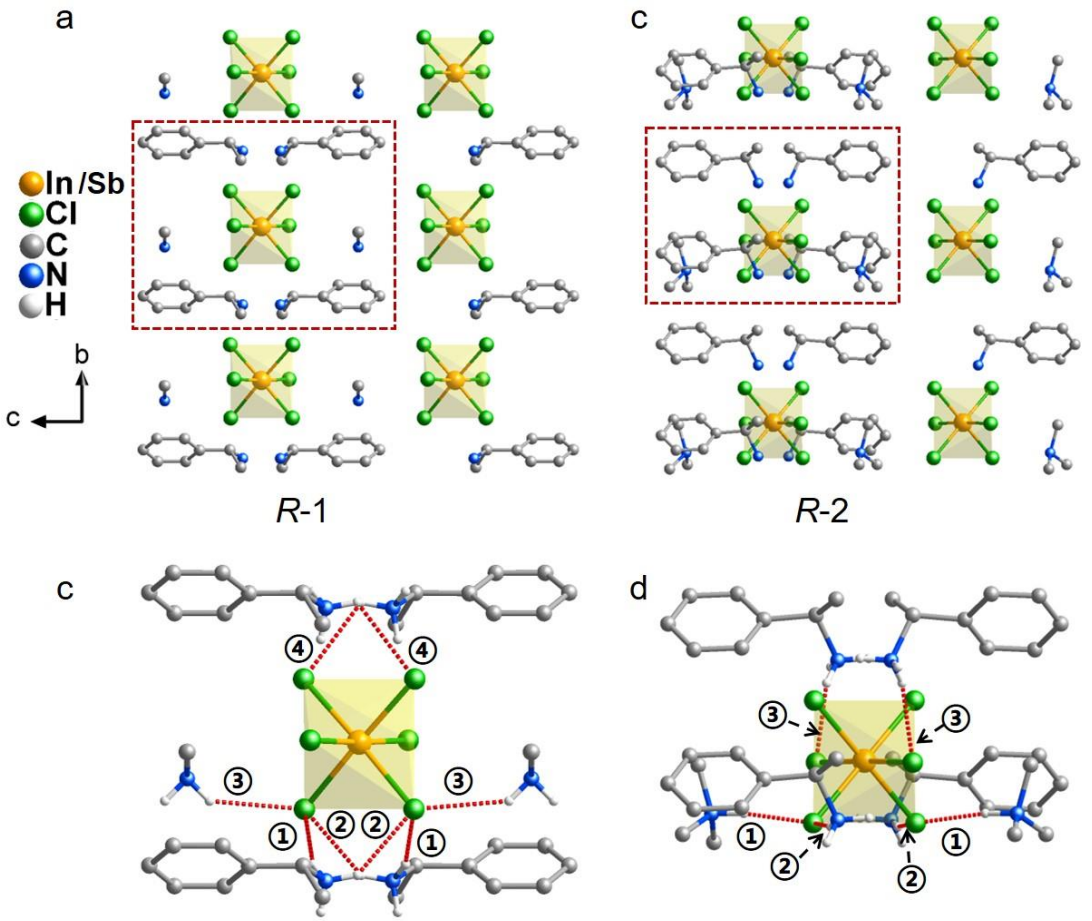

Figure S2. (a-b) Schematic crystal structure of *R*-1 and *R*-2 viewed from the a-axis, respectively. (c-d) Hydrogen bonds between organic ligands and inorganic octahedra of *R*-1 and *R*-2 viewed from the a-axis, respectively.

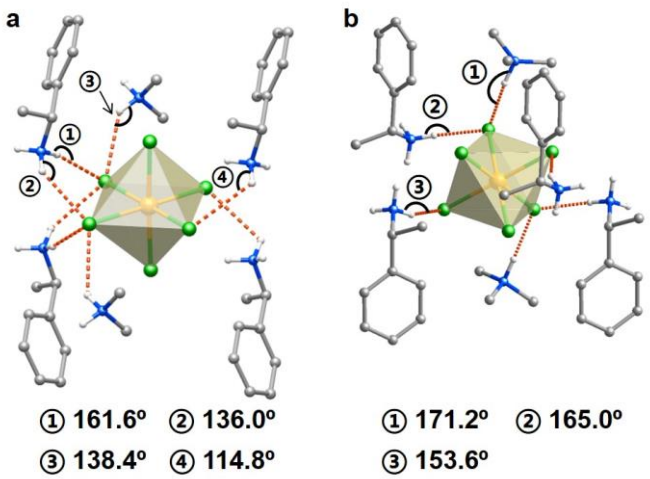

Figure S3. N-H···Y angles in *R*-1 (a) and *R*-2 (b).

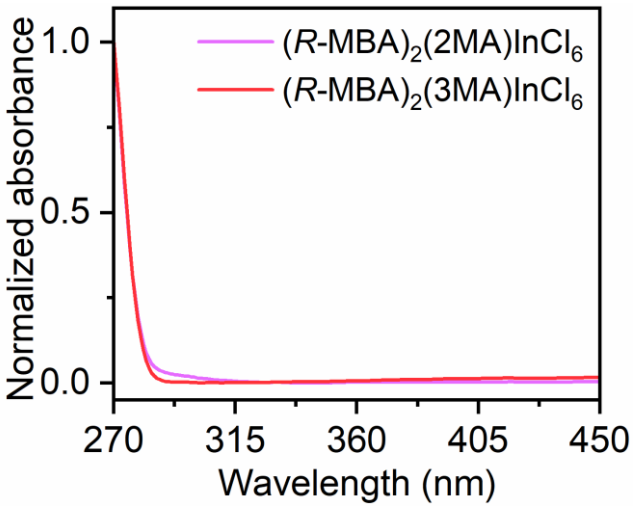

Figure S4. Normalized UV-Vis absorption spectra of (*R*-MBA)$_2$(2MA)InCl$_6$ and (*R*-MBA)$_2$(3MA)InCl$_6$.

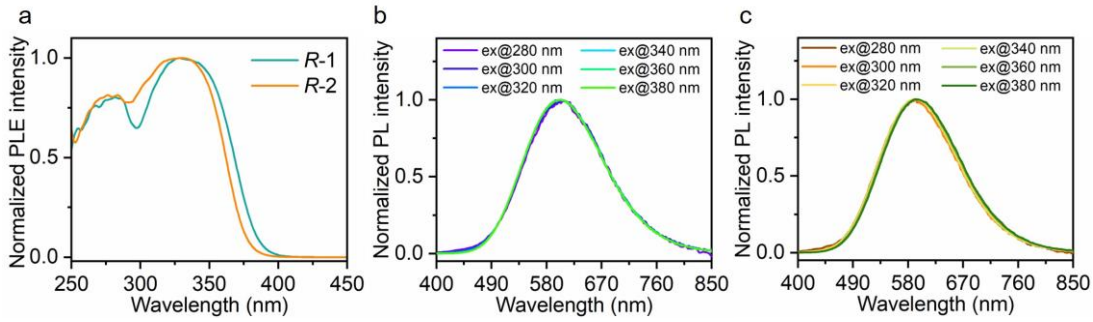

Figure S5. (a) Normalized PLE spectra of *R*-1 and *R*-2. (b-c) Normalized excitation-dependent PL spectra of *R*-1 and *R*-2, respectively.

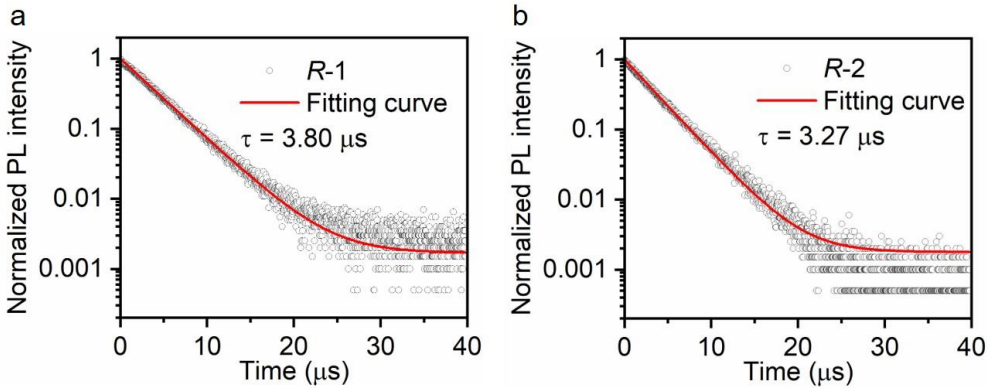

Figure S6. (a-b) Normalized time-resolved decay curves of *R*-1 and *R*-2, respectively.

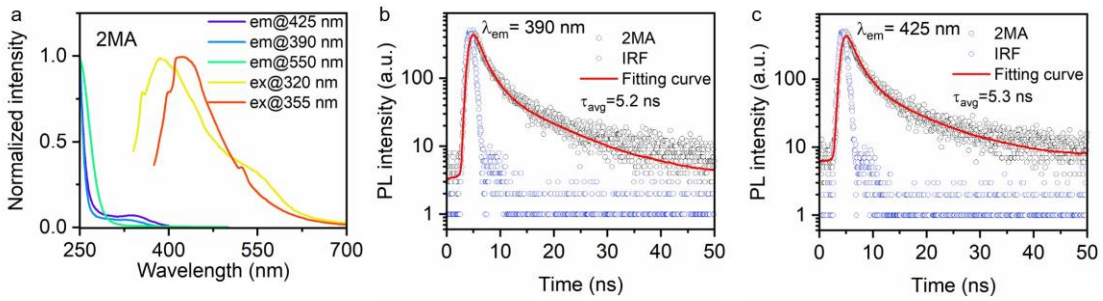

Figure S7. (a) Normalized PL and PLE spectra of 2MA. (b-c) Time-resolved decay curves of 2MA. IRF: instrument response function.

The PL spectra of 2MA exhibit two emissions mainly centered at 390 and 425 nm, respectively. The corresponding PL lifetimes are estimated to be 5.2 ns and 5.3 ns, respectively. While 3MA shows no emission under any excitation wavelengths. PL spectra and lifetimes of *R*-MBACl ligands have been previously reported, demonstrating an excitation-dependent emission. Moreover, the PL lifetimes of *R*-MBACl are estimated to be around 2.4 ns at 390 nm and 2.6 ns at 448 nm, respectively.[3]

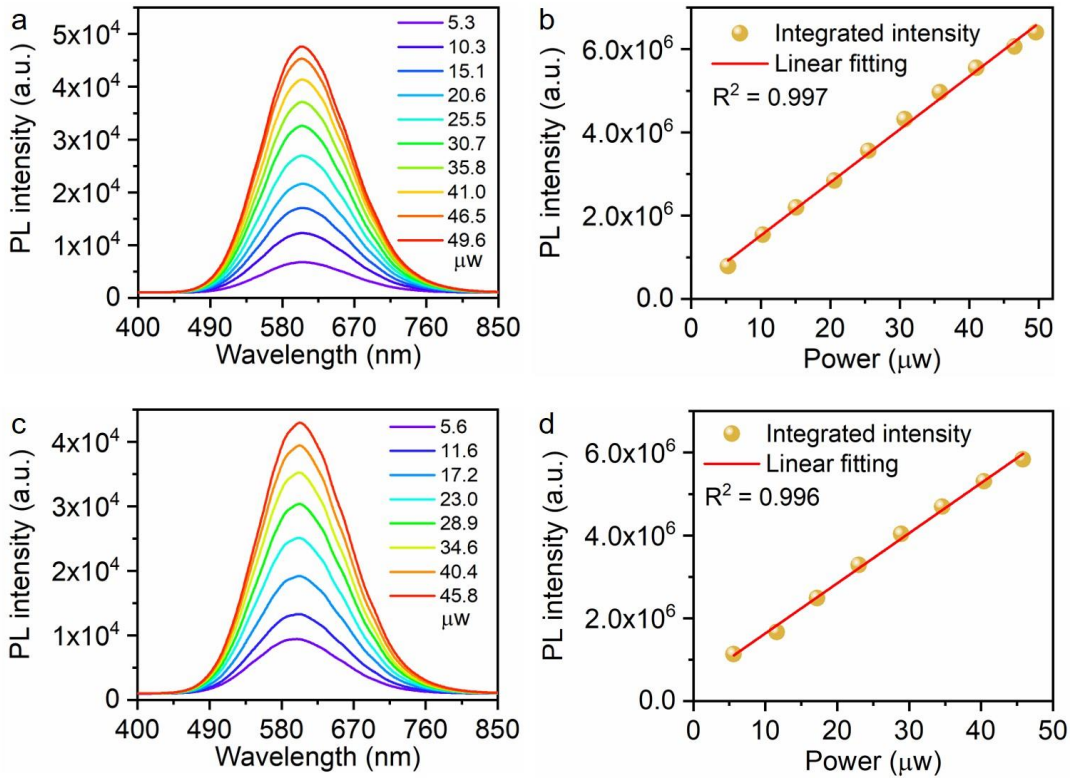

Figure S8. (a-b) Power-dependent PL spectra of *R*-1 and *R*-2, respectively. Variation of the emission intensities of *R*-1 (c) and *R*-2 (d) as a function of the excitation power.

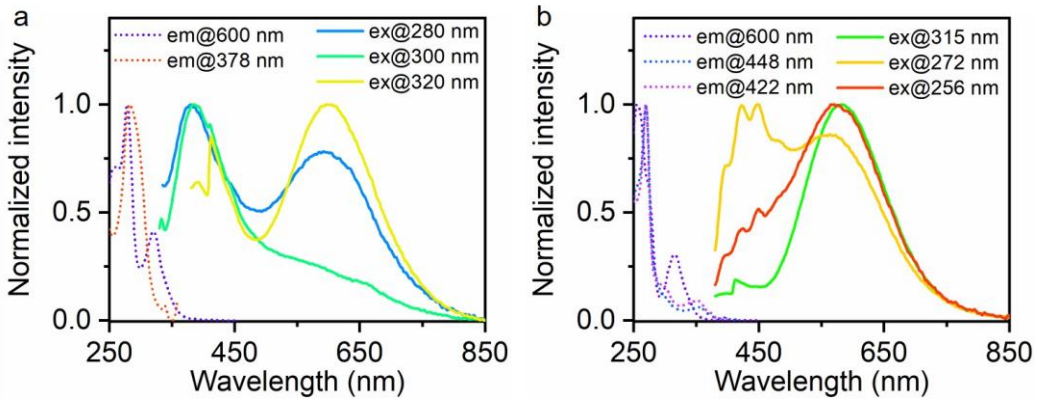

Figure S9. Normalized PL and PLE spectra of (*R*-MBA)$_2$(2MA)InCl$_6$ (a) and (*R*-MBA)$_2$(3MA)InCl$_6$ (b).

(*R*-MBA)$_2$(2MA)InCl$_6$ shows two emissions peaked at 378 and 600 nm, respectively. The PLE spectra of (*R*-MBA)$_2$(2MA)InCl$_6$ are located in the range of 250-400 nm with two peaks centered at 280 and 320 nm, respectively. Similarly, the PL spectra of (*R*-MBA)$_2$(3MA)InCl$_6$ exhibit two emissions centered at 448 and 600 nm. The PLE peaks mainly locate at 272 and 315 nm.

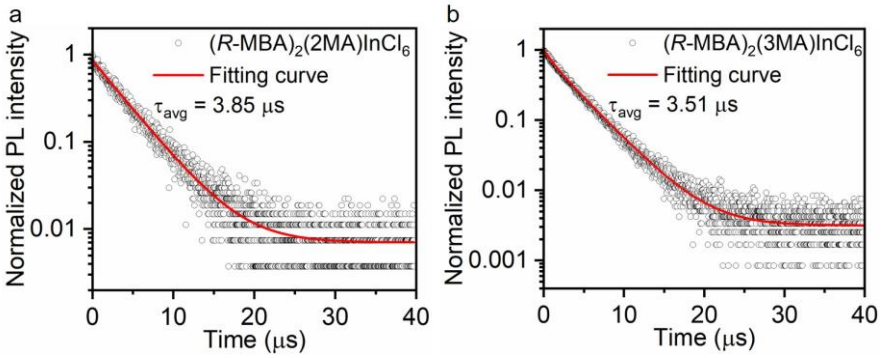

Figure S10. (a-b) Normalized time-resolved decay curves of (*R*-MBA)$_2$(2MA)InCl$_6$ and (*R*-MBA)$_2$(3MA)InCl$_6$, respectively.

Time-resolved decay curves of (*R*-MBA)$_2$(2MA)InCl$_6$ monitored at 378 nm and (*R*-MBA)$_2$(3MA)InCl$_6$ monitored at 448 nm are too weak to detect under 280 EPL-LED.

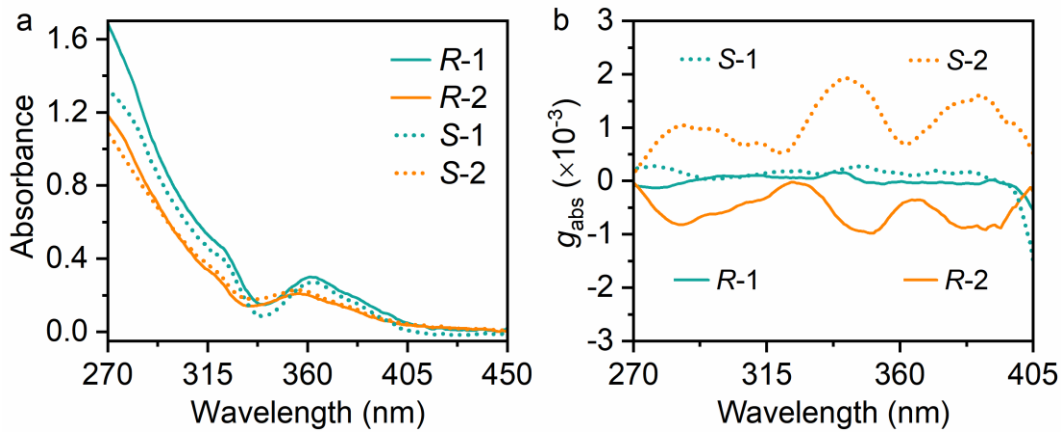

Figure S11. (a) UV-Vis absorption spectra obtained from CD measurements. (b) Calculated g_{abs} from CD spectra.

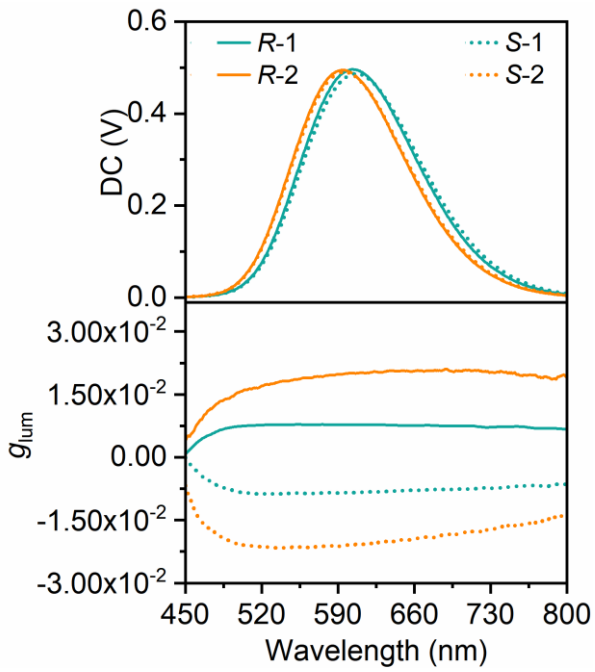

Figure S12. DC (top) and g_{lum} (down) spectra of *R*/*S*-1 and *R*/*S*-2. The maximum DC voltages are set to be about 0.5V. The wavelengths of maximum voltage are consistent with their corresponding PL emission center.

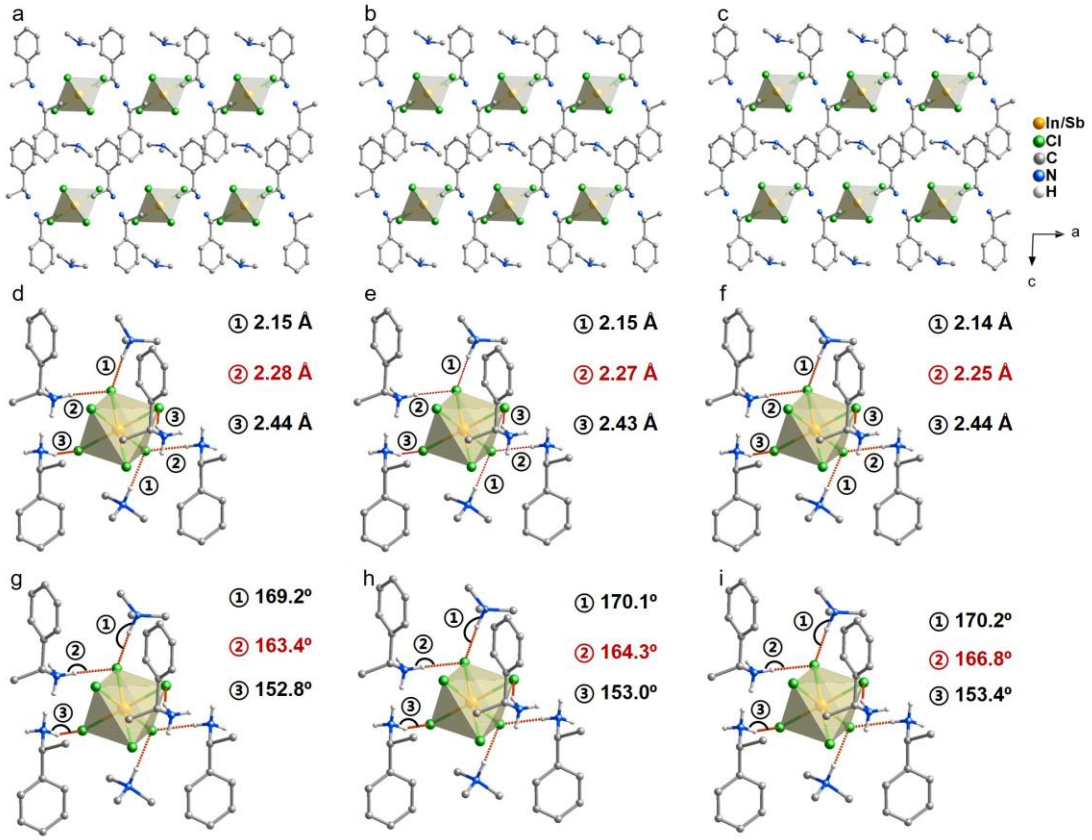

Figure S13. Schematic crystal structures (a-c), the H···Cl distance (d-f) and the N-H···Cl angle (g-i) between ligands and octahedra of *R*-2A, *R*-2B and *R*-2C, respectively.

R-2A, *R*-2B and *R*-2C show similar crystal structure and hydrogen bond distribution.

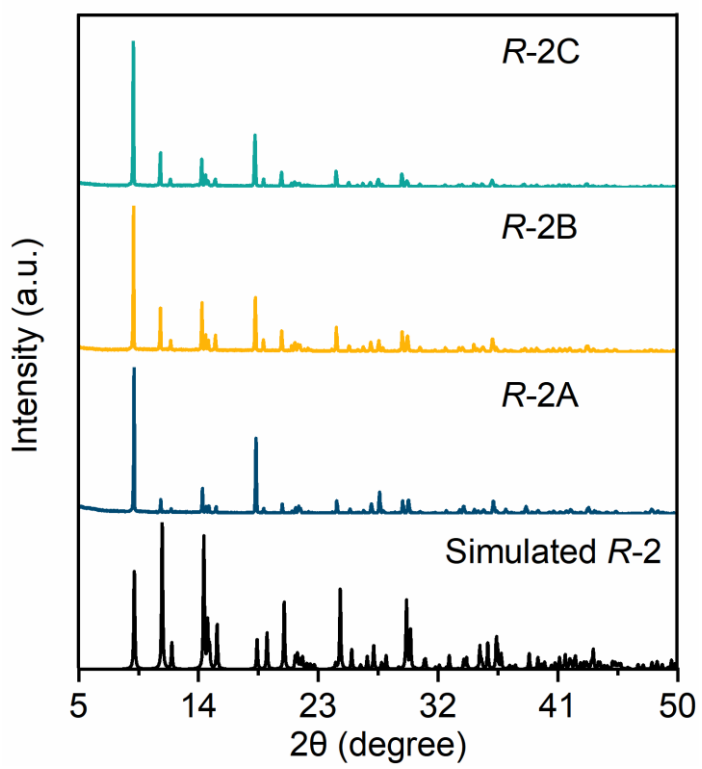

Figure S14. Experimental and simulated PXRD patterns of *R*-2A, *R*-2B and *R*-2C.

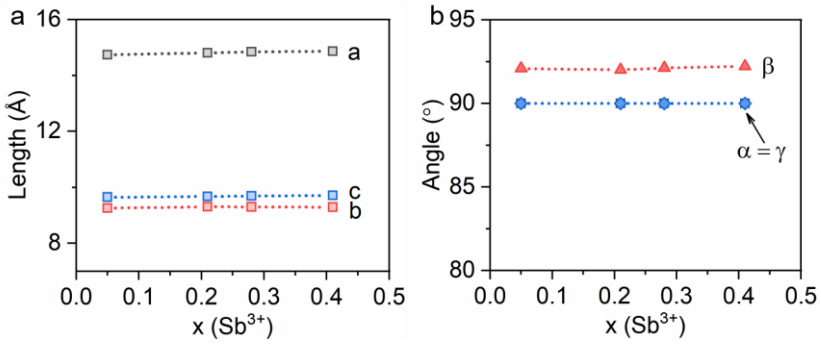

Figure S15. Variation of unit cell lattice constants (a) and angles (b) as a function of the Sb^{3+} concentration.

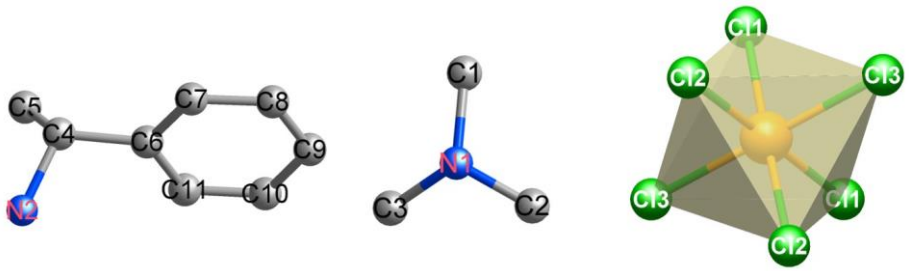

Figure S16. Organic ligands and inorganic octahedra with atom labels.

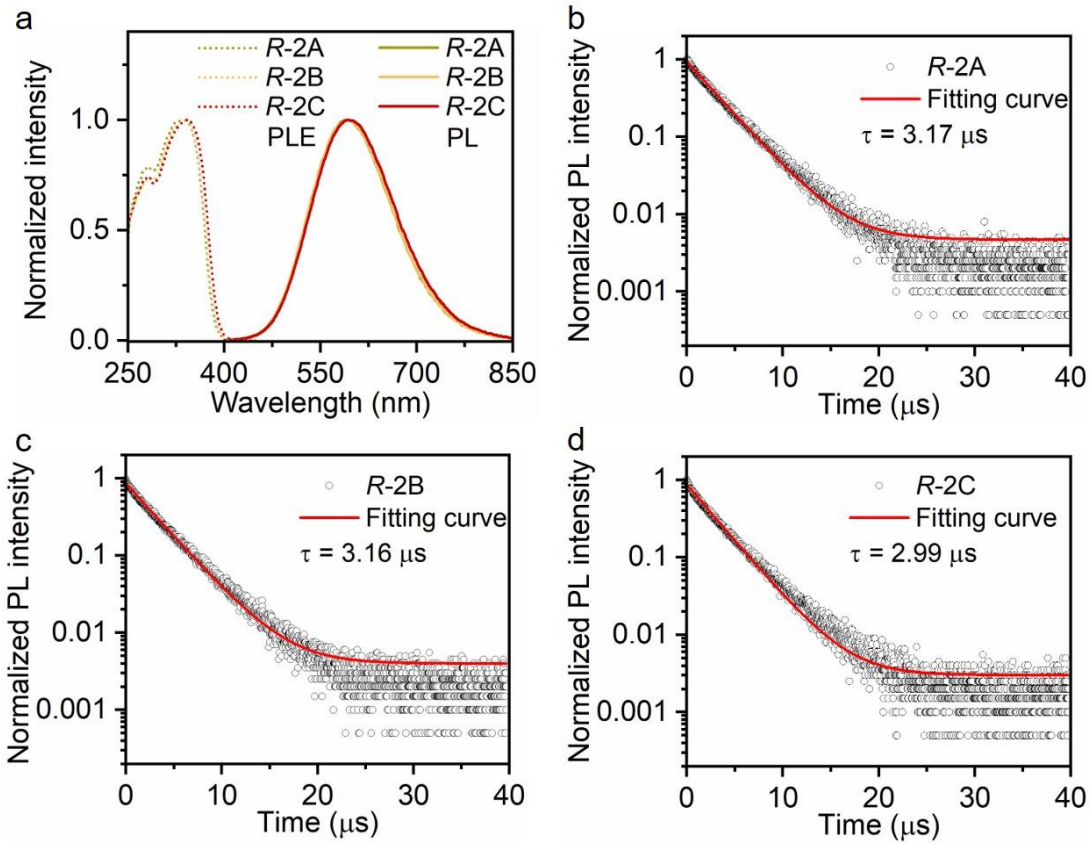

Figure S17. (a) Normalized PL and PLE spectra of *R*-2A, *R*-2B and *R*-2C. (b-c) Normalized time-resolved decay curves of *R*-2A, *R*-2B and *R*-2C, respectively.

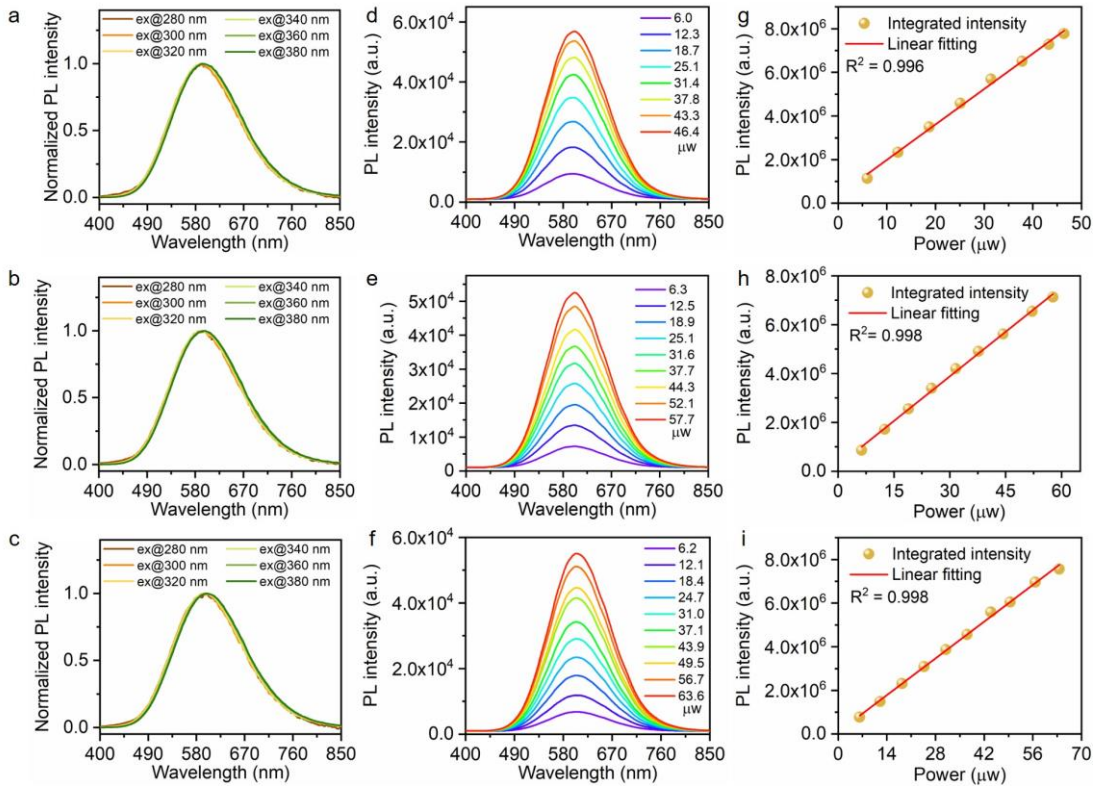

Figure S18. (a-c) Wavelength-dependent PL spectra of *R*-2A, *R*-2B and *R*-2C, respectively. (d-f) Power-dependent PL spectra of *R*-2A, *R*-2B and *R*-2C, respectively. (g-i) PL intensity versus excitation power of *R*-2A, *R*-2B and *R*-2C, respectively.

The microsecond lifetimes, unvaried wavelength-dependent PL spectra and linearly fitted power-dependent data of *R*-2A, *R*-2B and *R*-2C demonstrate that the bright emission originates from Sb^{3+}.

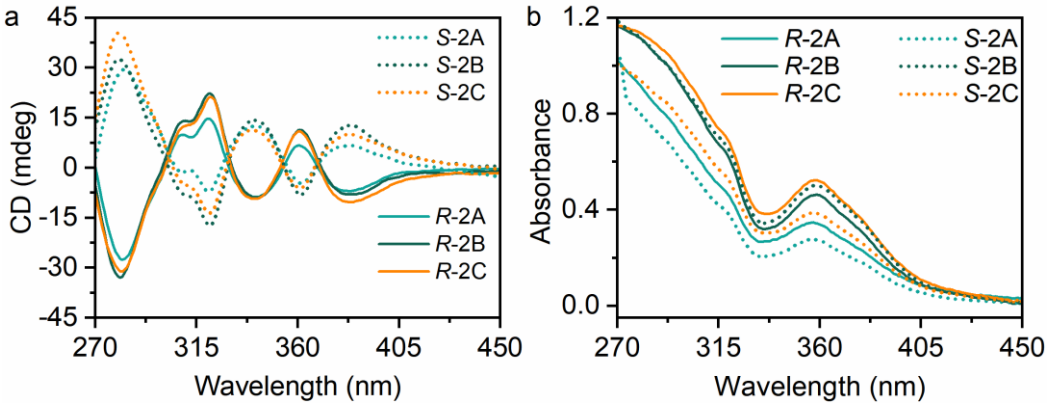

Figure S19. (a-b) CD, absorption and g_{abs} spectra of *R*/*S*-2A, *R*/*S*-2B and *R*/*S*-2C, respectively.

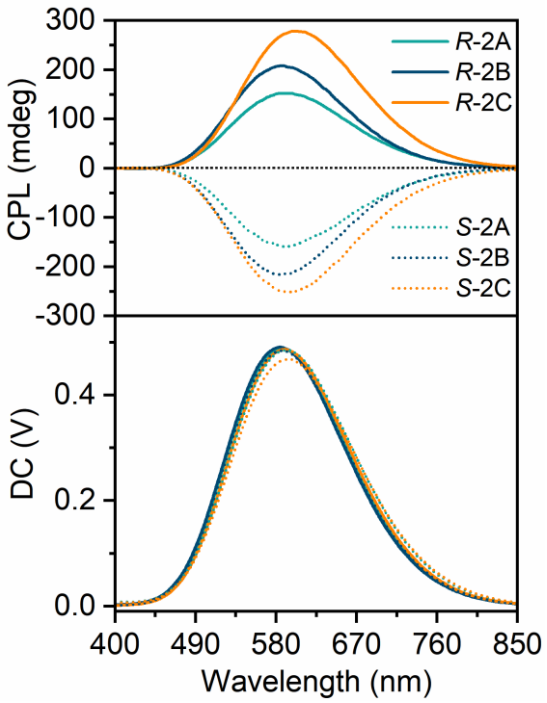

Figure S20. CPL spectra (top) and DC (down) spectra of *R*-2A, *R*-2B and *R*-2C.

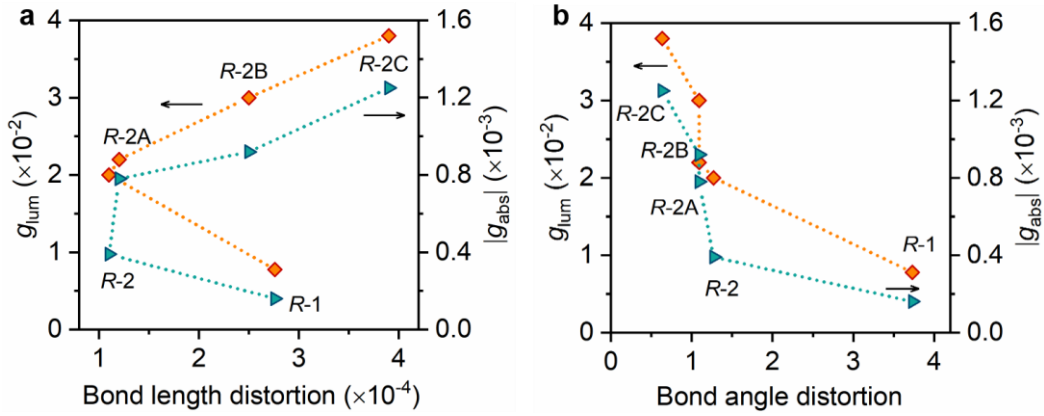

Figure S21. Plots of $|g_{abs}|$ and g_{lum} values as a function of bond length (a) and bond angle distortions (b) in these compounds.

Supplementary tables

Table S1: The result of ICP-MS measurements of *R*-1 and *R*-2.

Sample	In/Sb molar feed ratio	Actual In concentration (μg/L)	Actual Sb concentration (μg/L)	Actual Sb/(In+Sb) molar ratio
R-1	1.44 : 0.06	558.69	28.32	0.05
R-2	1.44 : 0.06	788.29	42.13	0.05

Table S2: Crystallographic data and structure refinements of *R*-1 and *R*-2.

Compound	*R*-1	*R*-2
Empirical formula	$C_{18}H_{31}Cl_6In_{0.95}Sb_{0.05}N_3$	$C_{19}H_{34}Cl_6In_{0.95}Sb_{0.05}N_3$
Formula weight	617.32	632.36
Temperature/K	100	100
Crystal system	monoclinic	monoclinic
Space group	*C*2	*C*2
a/Å	17.626(2)	14.740(6)
b/Å	7.5830(9)	9.260(4)
c/Å	9.5983(11)	9.647(4)
α/°	90	90
β/°	93.496(5)	92.088(13)
γ/°	90	90
Volume/Å^3	1280.5(3)	1315.9(9)
Z	2	2
ρ_{calc} g/cm^3	1.601	1.596
μ/mm^{-1}	1.567	1.527
F(000)	622.0	640.0
Crystal size/mm^3	0.1 × 0.1 × 0.1	0.1 × 0.1 × 0.1
Radiation	MoKα (λ = 0.71073)	MoKα (λ = 0.71073)
2θ range for data collection/°	7.15 to 54.968	5.196 to 55.224
Reflections collected	11261	12920
Independent reflections	2907 [R_{int} = 0.0423, R_{sigma} = 0.0376]	3030 [R_{int} = 0.0662, R_{sigma} = 0.0513]
Data/restraints/parameters	2907/1/131	3030/4/145
Goodness-of-fit on F^2	1.052	1.057
Final R indexes [I>=2σ (I)]	R_1 = 0.0295, wR_2 = 0.0592	R_1 = 0.0305, wR_2 = 0.0705
Final R indexes [all data]	R_1 = 0.0326, wR_2 = 0.0611	R_1 = 0.0345, wR_2 = 0.0748
Largest diff. peak/hole / e Å^{-3}	0.52/-0.56	0.67/-0.91
Flack parameter	0.01 (2)	0.06 (2)
CCDC	2344292	2344293

Table S3: Bond length and bond angle distortion of *R*-1 and *R*-2

Sample	Bond length distortion $(\Delta d)^1$	Bond angle distortion $(\sigma^2)^2$
R-1	2.76×10^{-4}	3.73
R-2	1.1×10^{-4}	1.27

[1] $\Delta d=\frac{1}{6}\sum\left[\frac{d_n-d}{d}\right]^2$, where d is the mean In/Sb−Cl bond length and d_n is the six individual In/Sb−Cl bond length.

[2] $\sigma^2=\frac{1}{11}\sum_{i=1}^{12}(\theta_i-90)^2$, where θ_i is the individual Cl−In/Sb−Cl angle.

Table S4: Crystallographic data and structure refinements of *R*-2A, *R*-2B, and *R*-2C.

Compound	*R*-2A	*R*-2B	*R*-2C
Empirical formula	$C_{19}H_{34}Cl_6In_{0.79}Sb_{0.21}N_3$	$C_{19}H_{34}Cl_6In_{0.72}Sb_{0.28}N_3$	$C_{19}H_{34}Cl_6In_{0.59}Sb_{0.41}N_3$
Formula weight	633.47	633.95	634.85
Temperature/K	100	100	100
Crystal system	monoclinic	monoclinic	monoclinic
Space group	*C*2	*C*2	*C*2
a/Å	14.807(5)	14.843(5)	14.863(4)
b/Å	9.305(3)	9.300(3)	9.290(2)
c/Å	9.672(4)	9.690(3)	9.706(2)
α/°	90	90	90
β/°	92.017(11)	92.129(11)	92.229(8)
γ/°	90	90	90
Volume/Å^3	1331.9(8)	1336.8(7)	1339.2(5)
Z	2	2	2
ρ_{calc} g/cm^3	1.580	1.575	1.574
μ/mm^{-1}	1.532	1.537	1.554
F(000)	641.0	641.0	642.0
Crystal size/mm^3	0.1 × 0.1 × 0.1	0.1 × 0.1 × 0.1	0.1 × 0.1 × 0.1
Radiation	MoKα (λ = 0.71073)	MoKα (λ = 0.71073)	MoKα (λ = 0.71073)
2θ range for data collection/°	5.506 to 55.002	5.17 to 54.994	5.486 to 54.97
Reflections collected	15386	15148	14885
Independent reflections	3029 [R_{int} = 0.0632, R_{sigma} = 0.0424]	3053 [R_{int} = 0.0646, R_{sigma} = 0.0449]	3071 [R_{int} = 0.0624, R_{sigma} = 0.0467]
Data/restraints/parameters	3029/22/152	3053/10/152	3071/10/152
Goodness-of-fit on F^2	1.080	1.091	1.070
Final R indexes [I>=2σ (I)]	R_1 = 0.0260, wR_2 = 0.0628	R_1 = 0.0280, wR_2 = 0.0594	R_1 = 0.0278, wR_2 = 0.0591
Final R indexes [all data]	R_1 = 0.0276, wR_2 = 0.0651	R_1 = 0.0322, wR_2 = 0.0626	R_1 = 0.0312, wR_2 = 0.0615
Largest diff. peak/hole / e Å^{-3}	0.45/-0.65	0.58/-0.74	0.41/-0.39
Flack parameter	0.05(3)	0.08(4)	0.07(3)
CCDC	2344294	2344295	2344296

Table S5: The result of ICP-MS measurements of *R*-2A, *R*-2B and *R*-2C.

Sample	In/Sb molar feed ratio	Actual In concentration (μg/L)	Actual Sb concentration (μg/L)	Actual Sb/(In+Sb) molar ratio
R-2A	1.28 : 0.22	554.12	156.49	0.21
R-2B	1.1 : 0.4	978.93	405.93	0.28
R-2C	1 : 0.5	713.67	521.26	0.41

Table S6: Lengths of N…Cl for *R*-2A, *R*-2B and *R*-2C.

Covalent bond	*R*-2A(Å)	*R*-2B (Å)	*R*-2C (Å)
N1…C11	3.139	3.137	3.128
N2…C11	3.159	3.154	3.145

Table S7: ICP results of *S*-1, *S*-2, *S*-2A, *S*-2B and *S*-2C.

Sample	In/Sb molar feed ratio	Actual In concentration (μg/L)	Actual Sb concentration (μg/L)	Actual Sb/(In+Sb) molar ratio
S-1	1.44 : 0.06	849.37	47.22	0.05
S-2	1.44 : 0.06	919.99	48.26	0.05
S-2A	1.28 : 0.22	1159.70	320.05	0.21
S-2B	1.1 : 0.4	1179.37	478.21	0.28
S-2C	1 : 0.5	575.89	421.06	0.41

Table S8: Reported g_{lum} values and PLQYs of chiral HMHs.

Samples	$\|g_{lum}\|$ ($\times 10^{-3}$)	PLQY (%)	Reference
R/*S*-$MnBr_3$	6.1	28.13/32.46	4
(*RR*/*SS*-DMPZ)$PbBr_4$	23.2	28.4	5
R/*S*-$(H_2MPz)_3PbBr_{10}$·2DMAc	3/3	16.38/14.18	6
(*R*-$C_5H_{14}N_2$)$PbBr_4$·H_2O	1.8	5.07	7
R-PbSnBr·H_2O	3	100	8
R/*S*-$C_6H_{15}Cl_2NO \cdot SbCl_5$	0.25/0.16	56.3/71.2	9
R/*S*-[MBA-Me_3]$MnBr_4$	4.5	100	10
DMA4[$InCl_6$] Br	5	81.4	11
R-$MGIn_{0.99}Sb_{0.01}Cl$	10	100	3
(*R*-CHEA)$_4In_{1.35}Sb_{0.65}Cl_{10}$	15	6.8	12
***R*-2C**	**38**	**100**	**This work**

Table S9: Bond lengths and bond angles for *R*-1. Bond lengths are reported with 2 significant figures in the main text.

Atom	Atom	Length（Å）	Atom	Atom	Length（Å）
Sb1	Cl1	2.535(2)	C4	C1	1.376(9)
Sb1	Cl1[1]	2.535(2)	C2	C3	1.395(6)
Sb1	Cl2[1]	2.4663(12)	C2	C1	1.363(8)
Sb1	Cl2	2.4663(12)	C6	C3	1.378(7)
Sb1	Cl3	2.566(2)	C6	C7	1.508(6)
Sb1	Cl3[1]	2.566(2)	C6	C5	1.386(7)
Cl1	In	2.535(2)	N1	C7	1.473(7)
Cl2	In	2.4663(12)	C7	C8	1.496(8)
Cl3	In	2.566(2)	C9	N2	1.427(8)
C4	C5	1.373(8)			

[1]1-X,+Y,1-Z

Atom	Atom	Atom	Angle（º）	Atom	Atom	Atom	Angle（º）
Cl1	Sb1	Cl1[1]	92.18(11)	N1	C7	C6	110.9(4)
Cl1	Sb1	Cl31	90.31(4)	N1	C7	C8	108.0(6)
Cl1	Sb1	Cl3	177.28(10)	C8	C7	C6	114.3(4)
Cl1[1]	Sb1	Cl3[1]	177.27(11)	C4	C5	C6	121.0(5)
Cl1[1]	Sb1	Cl3	90.31(4)	C2	C1	C4	119.8(5)
Cl2	Sb1	Cl1	90.11(10)	C9	N2	C9[2]	117.4(10)
Cl2	Sb1	Cl1[1]	88.08(10)	Cl1	In	Cl1[1]	92.18(11)
Cl2[1]	Sb1	Cl1	88.07(10)	Cl1	In	Cl3	177.28(10)
Cl2[1]	Sb1	Cl1[1]	90.11(10)	Cl1	In	Cl3[1]	90.31(4)
Cl2[1]	Sb1	Cl2	177.4(2)	Cl1[1]	In	Cl3	90.31(4)
Cl2[1]	Sb1	Cl3	93.02(11)	Cl1[1]	In	Cl3[1]	177.27(11)
Cl2	Sb1	Cl3	88.87(11)	Cl2	In	Cl1	90.11(10)
Cl2[1]	Sb1	Cl3[1]	88.87(11)	Cl2	In	Cl1[1]	88.08(10)
Cl2	Sb1	Cl3[1]	93.02(11)	Cl2[1]	In	Cl1	88.07(10)
Cl3[1]	Sb1	Cl3	87.22(11)	Cl2[1]	In	Cl1[1]	90.11(10)
C5	C4	C1	120.2(5)	Cl2[1]	In	Cl2	177.4(2)
C1	C2	C3	120.2(6)	Cl2[1]	In	Cl3[1]	88.87(11)
C3	C6	C7	123.8(4)	Cl2	In	Cl3	88.87(11)
C3	C6	C5	118.3(4)	Cl2	In	Cl3[1]	93.02(11)
C5	C6	C7	117.9(4)	Cl2[1]	In	Cl3	93.02(11)
C6	C3	C2	120.5(5)	Cl3[1]	In	Cl3	87.22(11)

[1]1-X,+Y,1-Z; [2]1-X,+Y,2-Z

Table S10: Bond lengths and bond angles for *R*-2. Bond lengths are reported with 2 significant figures in the main text.

Atom	Atom	Length（Å）	Atom	Atom	Length（Å）
Sb1	Cl2	2.486(2)	C5	C4	1.510(8)
Sb1	Cl2[1]	2.486(2)	C7	C6	1.382(8)
Sb1	Cl3[1]	2.5467(13)	C6	C11	1.397(7)
Sb1	Cl3	2.5467(13)	C6	C4	1.517(7)
Sb1	Cl1	2.535(2)	N2	C4	1.509(7)
Sb1	Cl1[1]	2.535(2)	C10	C11	1.385(8)
Cl2	In1A	2.486(2)	C10	C9	1.376(9)
Cl3	In1A	2.5467(13)	C2	N1	1.481(16)
C1	N1	1.470(13)	N1	C3	1.470(18)
C8	C7	1.387(7)	Cl1	In1A	2.535(2)
C8	C9	1.373(9)			

[1]-X,+Y,-Z

Atom	Atom	Atom	Angle（°）	Atom	Atom	Atom	Angle（°）
Cl2	Sb1	Cl2[1]	90.69(10)	C8	C9	C10	119.6(5)
Cl2[1]	Sb1	Cl3	91.74(7)	C5	C4	C6	113.9(4)
Cl2	Sb1	Cl3	89.86(7)	N2	C4	C5	108.8(5)
Cl2[1]	Sb1	Cl3[1]	89.86(7)	N2	C4	C6	110.1(4)
Cl2	Sb1	Cl3[1]	91.74(7)	C1	N1	C2	107.3(14)
Cl2	Sb1	Cl1	178.72(10)	C3	N1	C1	119.0(13)
Cl2	Sb1	Cl1[1]	90.04(4)	C3	N1	C2	112.8(10)
Cl2[1]	Sb1	Cl1[1]	178.72(10)	Cl2	In1A	Cl2[1]	90.69(10)
Cl2[1]	Sb1	Cl1	90.04(4)	Cl2[1]	In1A	Cl3	91.74(7)
Cl3	Sb1	Cl3[1]	177.73(12)	Cl2	In1A	Cl3[1]	91.74(7)
Cl1[1]	Sb1	Cl3	89.32(7)	Cl2	In1A	Cl3	89.86(7)
Cl1[1]	Sb1	Cl3[1]	89.06(7)	Cl2[1]	In1A	Cl3[1]	89.86(7)
Cl1	Sb1	Cl3	89.06(7)	Cl2[1]	In1A	Cl1	90.04(7)
Cl1	Sb1	Cl3[1]	89.32(7)	Cl2[1]	In1A	Cl1[1]	178.72(10)
Cl1	Sb1	Cl1[1]	89.25(10)	Cl2	In1A	Cl1	178.72(10)
C9	C8	C7	120.5(6)	Cl2	In1A	Cl1[1]	90.04(4)
C6	C7	C8	120.5(6)	Cl3	In1A	Cl3[1]	177.73(12)
C7	C6	C11	118.8(5)	Cl1	In1A	Cl3[1]	89.32(7)
C7	C6	C4	119.9(5)	Cl1[1]	In1A	Cl3[1]	89.06(7)
C11	C6	C4	121.2(5)	Cl1	In1A	Cl3	89.06(7)
C9	C10	C11	120.5(5)	Cl1[1]	In1A	Cl3	89.32(7)
C10	C11	C6	120.1(5)	Cl1	In1A	Cl1[1]	89.25(10)

[1]-X,+Y,-Z

Table S11: Bond lengths and bond angles for *R*-2A. Bond lengths are reported with 2 significant figures in the main text.

Atom	Atom	Length（Å）	Atom	Atom	Length（Å）
Sb1	Cl1	2.5621(19)	C8	C7	1.392(6)
Sb1	Cl1[1]	2.5621(19)	C8	C9	1.379(7)
Sb1	Cl3[1]	2.5638(10)	C7	C6	1.388(6)
Sb1	Cl3	2.5638(10)	N2	C4	1.510(5)
Sb1	Cl2[1]	2.5008(16)	C11	C10	1.390(7)
Sb1	Cl2	2.5008(16)	C11	C6	1.392(6)
Cl1	In1A	2.5621(19)	C4	C6	1.517(6)
Cl3	In1A	2.5638(10)	C9	C10	1.386(7)
Cl2	In1A	2.5008(16)	C2	N1	1.46(3)
C5	C4	1.515(6)	N1	C3	1.49(3)
C1	N1	1.477(13)			

[1]-X,+Y,-Z

Atom	Atom	Atom	Angle（°）	Atom	Atom	Atom	Angle（°）
Cl1	Sb1	Cl1[1]	89.57(8)	C9	C10	C11	120.5(4)
Cl1[1]	Sb1	Cl3[1]	89.37(6)	C7	C6	C11	119.3(4)
Cl1[1]	Sb1	Cl3	89.31(6)	C7	C6	C4	119.3(4)
Cl1	Sb1	Cl3[1]	89.31(6)	C11	C6	C4	121.4(4)
Cl1	Sb1	Cl3	89.37(6)	C1	N1	C3	109.5(11)
Cl3	Sb1	Cl3[1]	178.14(10)	C2	N1	C1	119.1(12)
Cl2	Sb1	Cl1[1]	90.10(4)	C2	N1	C3	113.9(11)
Cl2[1]	Sb1	Cl1	90.10(4)	Cl1	In1A	Cl1[1]	89.57(8)
Cl2[1]	Sb1	Cl1[1]	178.86(8)	Cl1	In1A	Cl3	89.37(6)
Cl2	Sb1	Cl1	178.86(8)	Cl1	In1A	Cl3[1]	89.31(6)
Cl2[1]	Sb1	Cl3[1]	89.54(6)	Cl1[1]	In1A	Cl3[1]	89.37(6)
Cl2[1]	Sb1	Cl3	91.77(6)	Cl1[1]	In1A	Cl3	89.31(6)
Cl2	Sb1	Cl3	89.54(6)	Cl3	In1A	Cl3[1]	178.14(10)
Cl2	Sb1	Cl3[1]	91.77(6)	Cl2[1]	In1A	Cl1	90.10(4)
Cl2[1]	Sb1	Cl2	90.26(8)	Cl2	In1A	Cl1	178.86(8)
C9	C8	C7	120.7(5)	Cl2	In1A	Cl1[1]	90.10(4)
C6	C7	C8	120.1(4)	Cl2[1]	In1A	Cl1[1]	178.86(8)
C10	C11	C6	120.1(4)	Cl2[1]	In1A	Cl3[1]	89.54(6)
C5	C4	C6	113.4(4)	Cl2	In1A	Cl3[1]	91.77(6)
N2	C4	C5	109.3(4)	Cl2	In1A	Cl3	89.54(6)
N2	C4	C6	110.2(3)	Cl2[1]	In1A	Cl3	91.77(6)
C8	C9	C10	119.3(4)	Cl2[1]	In1A	Cl2	90.26(8)

[1]-X,+Y,-Z

Table S12: Bond lengths and bond angles for *R*-2B. Bond lengths are reported with 2 significant figures in the main text.

Atom	Atom	Length（Å）	Atom	Atom	Length（Å）
Sb1	Cl2[1]	2.5049(18)	C4	N2	1.512(6)
Sb1	Cl2	2.5049(18)	C6	C7	1.386(7)
Sb1	Cl1[1]	2.587(2)	C6	C11	1.394(6)
Sb1	Cl1	2.587(2)	C7	C8	1.392(6)
Sb1	Cl3[1]	2.5802(11)	C8	C9	1.376(8)
Sb1	Cl3	2.5802(11)	C9	C10	1.386(7)
Cl2	In1A	2.5049(18)	C11	C10	1.387(7)
Cl1	In1A	2.587(2)	C1	N1	1.489(15)
Cl3	In1A	2.5802(11)	C3	N1	1.53(3)
C4	C6	1.516(6)	N1	C2	1.39(4)
C4	C5	1.515(7)			

[1]1-X,+Y,1-Z

Atom	Atom	Atom	Angle（º）	Atom	Atom	Atom	Angle（º）
Cl2[1]	Sb1	Cl2	90.05(9)	C9	C8	C7	120.8(5)
Cl2[1]	Sb1	Cl1	89.96(4)	C8	C9	C10	119.2(5)
Cl2[1]	Sb1	Cl1[1]	179.02(9)	C10	C11	C6	120.2(4)
Cl2	Sb1	Cl1	179.02(9)	C9	C10	C11	120.6(5)
Cl2	Sb1	Cl1[1]	89.96(4)	C1	N1	C3	112.5(14)
Cl2[1]	Sb1	Cl3[1]	89.27(7)	C2	N1	C1	115.4(12)
Cl2	Sb1	Cl3	89.27(7)	C2	N1	C3	113.9(12)
Cl2[1]	Sb1	Cl3	91.58(7)	Cl2[1]	In1A	Cl2	90.05(9)
Cl2	Sb1	Cl3[1]	91.58(7)	Cl2	In1A	Cl1[1]	89.96(4)
Cl1[1]	Sb1	Cl1	90.05(9)	Cl2[1]	In1A	Cl1[1]	179.02(9)
Cl3[1]	Sb1	Cl1[1]	89.74(6)	Cl2[1]	In1A	Cl1	89.96(4)
Cl3[1]	Sb1	Cl1	89.40(7)	Cl2	In1A	Cl1	179.02(9)
Cl3	Sb1	Cl1	89.74(6)	Cl2[1]	In1A	Cl3[1]	89.27(7)
Cl3	Sb1	Cl1[1]	89.40(7)	Cl2	In1A	Cl3[1]	91.58(7)
Cl3[1]	Sb1	Cl3	178.79(12)	Cl2[1]	In1A	Cl3	91.58(7)
C5	C4	C6	113.5(4)	Cl2	In1A	Cl3	89.27(7)
N2	C4	C6	110.0(4)	Cl1[1]	In1A	Cl1	90.05(9)
N2	C4	C5	109.6(5)	Cl3[1]	In1A	Cl1	89.40(7)
C7	C6	C4	119.3(4)	Cl3	In1A	Cl1	89.74(6)
C7	C6	C11	119.0(4)	Cl3[1]	In1A	Cl1[1]	89.74(6)
C11	C6	C4	121.6(4)	Cl3	In1A	Cl1[1]	89.40(7)
C6	C7	C8	120.2(5)	Cl3[1]	In1A	Cl3	178.79(12)

[1]1-X,+Y,1-Z

Table S13: Bond lengths and bond angles for *R*-2C. Bond lengths are reported with 2 significant figures in the main text.

Atom	Atom	Length（Å）	Atom	Atom	Length（Å）
Sb1	Cl1	2.5015(17)	C8	C9	1.379(7)
Sb1	Cl1[1]	2.5015(17)	C7	C6	1.379(6)
Sb1	Cl2[1]	2.619(2)	N2	C4	1.506(6)
Sb1	Cl2	2.619(2)	C6	C4	1.513(6)
Sb1	Cl3[1]	2.5934(10)	C6	C11	1.399(6)
Sb1	Cl3	2.5933(10)	C11	C10	1.379(7)
Cl1	In1A	2.5015(17)	C10	C9	1.387(7)
Cl2	In1A	2.619(2)	C2	N1	1.40(4)
C1	N1	1.491(13)	N1	C3	1.51(4)
C5	C4	1.518(7)	Cl3	In1A	2.5933(10)
C5	C7	1.394(6)			

[1]1-X,+Y,1-Z

Atom	Atom	Atom	Angle（º）	Atom	Atom	Atom	Angle（º）
Cl1	Sb1	Cl1[1]	89.75(8)	C6	C4	C5	113.6(4)
Cl1	Sb1	Cl2	178.99(8)	C10	C11	C6	120.2(4)
Cl1	Sb1	Cl2[1]	89.74(3)	C11	C10	C9	121.0(5)
Cl1[1]	Sb1	Cl2	89.74(3)	C8	C9	C10	118.8(5)
Cl1[1]	Sb1	Cl2[1]	178.99(8)	C1	N1	C3	112.9(17)
Cl1	Sb1	Cl3	91.52(6)	C2	N1	C1	114.2(14)
Cl1[1]	Sb1	Cl3	89.25(6)	C2	N1	C3	113.7(16)
Cl1[1]	Sb1	Cl3[1]	91.52(6)	Cl1	In1A	Cl1[1]	89.75(8)
Cl1	Sb1	Cl3[1]	89.25(6)	Cl1[1]	In1A	Cl2[1]	178.99(8)
Cl2	Sb1	Cl2[1]	90.78(9)	Cl1	In1A	Cl2[1]	89.74(3)
Cl3[1]	Sb1	Cl2	89.89(6)	Cl1[1]	In1A	Cl2	89.74(3)
Cl3	Sb1	Cl2[1]	89.89(6)	Cl1	In1A	Cl2	178.99(8)
Cl3[1]	Sb1	Cl2[1]	89.35(6)	Cl1[1]	In1A	Cl3	89.25(6)
Cl3	Sb1	Cl2	89.35(6)	Cl1	In1A	Cl3	91.52(6)
Cl3	Sb1	Cl3[1]	178.92(11)	Cl1[1]	In1A	Cl3[1]	91.52(6)
C9	C8	C7	120.5(5)	Cl1	In1A	Cl3[1]	89.25(6)
C6	C7	C8	120.7(5)	Cl2	In1A	Cl2[1]	90.78(9)
C7	C6	C4	119.6(4)	Cl3	In1A	Cl2[1]	89.89(6)
C7	C6	C11	118.7(4)	Cl3[1]	In1A	Cl2	89.89(6)
C11	C6	C4	121.6(4)	Cl3[1]	In1A	Cl2[1]	89.35(6)
N2	C4	C5	109.1(4)	Cl3	In1A	Cl2	89.35(6)
N2	C4	C6	110.1(3)	Cl3	In1A	Cl3[1]	178.92(11)

[1]-X,+Y,-Z

Supplementary references

1. O. V. Dolomanov, L. J. Bourhis, R. J. Gildea, J. A. K. Howard and H. Puschmann, OLEX2: a complete structure solution, refinement and analysis program, *J. Appl. Crystallogr.*, 2009, **42**, 339-341.
2. G. M. Sheldrick, SHELXT-Integrated space-group and crystal-structure determination, *Acta Crystallogr A*, 2015, **71**, 3-8.
3. Y. L. Liu, Z. S. Luo, Y. Wei, C. Li, Y. L. Chen, X. He, X. Y. Chang and Z. W. Quan, Integrating Achiral and Chiral Organic Ligands in Zero-Dimensional Hybrid Metal Halides to Boost Circularly Polarized Luminescence, *Angew. Chem., Int. Ed.*, 2023, **62**, e202306821.
4. J. X. Gao, W. Y. Zhang, Z. G. Wu, Y. X. Zheng and D. W. Fu, Enantiomorphic Perovskite Ferroelectrics with Circularly Polarized Luminescence, *J. Am. Chem. Soc.*, 2020, **142**, 4756-4761.
5. C. Y. Chai, Q. K. Zhang, C. Q. Jing, X. B. Han, C. D. Liu, B. D. Liang, C. C. Fan, Z. Chen, X. W. Lei, A. Stroppa, R. O. Agbaoye, G. A. Adebayo, C. F. Zhang and W. Zhang, Single-Component White Circularly Polarized Luminescence in Chiral 1D Double-Chain Perovskites, *Adv. Opt. Mater.*, 2023, **11**, 2201996.
6. K. H. Jin, Y. Zhang, K. J. Li, M. E. Sun, X. Y. Dong, Q. L. Wang and S. Q. Zang, Enantiomorphic Single Crystals of Linear Lead(II) Bromide Perovskitoids with White Circularly Polarized Emission, *Angew. Chem., Int. Ed.*, 2022, **61**, e202205317.
7. Y. Peng, X. Wang, L. N. Li, H. Ye, S. Yang, H. G. Yang, J. H. Luo and Y. Hou, Moisture-Resistant Chiral Perovskites for White-Light Circularly Polarized Photoluminescence, *Adv. Opt. Mater.*, 2023, **11**, 2201888.
8. Y. Wei, C. Li, Y. W. Li, Z. S. Luo, X. Y. Wu, Y. L. Liu, L. M. Zhang, X. He, W. Wang and Z. W. Quan, Circularly Polarized Luminescence from Zero-Dimensional Hybrid Lead-Tin Bromide with Near-Unity Photoluminescence Quantum Yield, *Angew. Chem., Int. Ed.*, 2022, **61**, e202212685.
9. H. L. Xuan, J. L. Li, L. J. Xu, D. S. Zheng and Z. N. Chen, Circularly Polarized Luminescence based on 0D Lead-Free Antimony (III) Halide Hybrids, *Adv. Opt. Mater.*, 2022, **10**, 2200591.
10. M. P. Davydova, L. Q. Meng, M. I. Rakhmanova, I. Y. Bagryanskaya, V. S. Sulyaeva, H. Meng and A. V. Artem'ev, Highly Emissive Chiral Mn(II) Bromide Hybrids for UV-Pumped Circularly Polarized LEDs and Scintillator Image Applications, *Adv. Opt. Mater.*, 2023, **11**, 2202811.
11. J. J. Guan, Y. S. Zheng, P. X. Cheng, W. Q. Han, X. Han, P. H. Wang, M. Y. Xin, R. C. Shi, J. L. Xu and X. H. Bu, Free Halogen Substitution of Chiral Hybrid Metal Halides for Activating the Linear and Nonlinear Chiroptical Properties, *J. Am. Chem. Soc.*, 2023, **145**, 26833-26842.
12. Z. Wang, X. Wang, Z. Chen, Y. Liu, H. Xie, J. Xue, L. Mao, Y. Yan and H. Lu, Turn-on Circularly Polarized Luminescence in Chiral Indium Chlorides by $5s^2$ Metal Centers, *Angew. Chem., Int. Ed.*, 2023, **62**, e202215206.